

igin for the loris-lemur clade cannot be ruled out (24) in the light of this new discovery. A similar scenario (adapted from molecular data) has been suggested for endemic Malagasy rodents (32).

The possibility that lemuriforms and lorisiforms originated in Asia rather than in Africa cannot be rejected without further paleontological evidence from both continents and from Madagascar. It must, however, be emphasized that their origin is undoubtedly as ancient as that of adapiforms (Fig. 3A). The discovery of a cheirogaleid-like lemur in Oligocene deposits of Pakistan suggests that whatever the timing and direction of faunal dispersions, South Asia was, as for anthropoids (33), an important theater of early strepsirrhine evolution, reflecting the complex role played by the drifting Greater India in the evolutionary history of Malagasy lemurs.

References and Notes

1. A. D. Yoder, M. Cartmill, M. Ruvolo, K. Smith, R. Vilgalys, *Proc. Natl. Acad. Sci. U.S.A.* **93**, 5122 (1996).
2. R. D. Martin, *Primate Origins and Evolution. A Phylogenetic Reconstruction* (Chapman & Hall, London, 1990).
3. R. D. E. MacPhee, L. L. Jacobs, in *Vertebrates, Phylogeny, and Philosophy*, K. M. Flanagan, K. A. Lillegraven, Eds. (Univ. of Wyoming, Laramie, WY, 1986), vol. 3, pp. 131–161.
4. T. D. Rasmussen, K. A. Nekaris, *Folia Primatol.* **69**, 250 (1998).
5. J.-L. Welcomme et al., *Geol. Mag.* **138**, 397 (2001).
6. E. Gheerbrant, H. Thomas, J. Roger, S. Sen, Z. Al-Sulaimani, *Palaeovertebrata* **22**, 141 (1993).
7. A. L. Rosenberger, E. Strasser, E. Delson, *Folia Primatol.* **44**, 15 (1985).
8. J. H. Schwartz, I. Tattersall, *Anthropol. Pap. Am. Mus. Nat. Hist.* **60**, 1 (1985).
9. C. K. Beard, M. Dagosto, D. L. Gebo, M. Godinot, *Nature* **331**, 712 (1988).
10. M. Dagosto, *J. Hum. Evol.* **17**, 35 (1988).
11. A. D. Yoder, *Evol. Anthropol.* **6**, 11 (1997).
12. P. Charles-Dominique, R. D. Martin, *Nature* **227**, 257 (1970).
13. F. S. Szalay, C. C. Katz, *Folia Primatol.* **19**, 88 (1973).
14. I. Tattersall, J. H. Schwartz, *Anthropol. Pap. Am. Mus. Nat. Hist.* **52**, 139 (1974).
15. M. Cartmill, in *Phylogeny of the Primates: A Multidisciplinary Approach*, W. P. Luckett, F. S. Szalay, Eds. (Plenum, New York, 1975), pp. 313–354.
16. M. Goodman et al., *Am. J. Phys. Anthropol.* **94**, 3 (1994).
17. A. D. Yoder, *Am. J. Phys. Anthropol.* **94**, 25 (1994).
18. W. K. Gregory, *Bull. Geol. Soc. Am.* **26**, 426 (1915).
19. A total of 169 dental characters have been compiled [see supplemental Web material (34)]. Most of the characters and state character types (ordered or unordered) are after Ross et al. (35). Morpho-anatomical characters for the DMAc analysis on living strepsirrhines are after Yoder (17) [from selected taxa, invariant characters have been removed; see supplemental Web material (34)]. Heuristic searches using stepwise addition and a randomized input order of taxa (100 replications) was performed by PAUP 3.1.1.
20. E. L. Simons, *Proc. Natl. Acad. Sci. U.S.A.* **94**, 180 (1997).
21. J. Pastorini, R. D. Martin, P. Ehresmann, E. Zimmermann, M. R. J. Forstner, *Mol. Phyl. Evol.* **19**, 45 (2001).
22. M. Storey et al., *Science* **267**, 852 (1995).
23. S. Kumar, S. B. Hedges, *Nature* **392**, 917 (1998).
24. R. D. Martin, *Folia Primatol.* **21**, 1021 (2000).
25. P. Jodot, *Mem. Inst. Sci. Madagascar* **D4**, 131 (1952).
26. P. M. Kappeler, *Folia Primatol.* **71**, 422 (2000).

27. R. A. McCall, *Proc. R. Soc. London Ser. B* **264**, 663 (1997).
28. P. D. Gingerich, in *Lemur Biology*, I. Tattersall, R. Sussman, Eds. (Plenum, New York, 1975), pp. 65–80.
29. R. L. Ciochon, D. A. Etler, in *Integrative Paths to the Past: Paleoanthropological Advances in Honor of F. Clark Howell*, R. S. Corruccini, R. L. Ciochon, Eds. (Prentice Hall, Englewood Cliffs, NJ, 1994), pp. 37–67.
30. J.-C. Rage, in *Biogéographie de Madagascar*, W. R. Lourenço, Ed. (Éditions ORSTOM, Paris, 1996), pp. 27–35.
31. P. D. Gingerich, *Geobios* **1**, 165 (1977).
32. S. A. Jansa, S. M. Goodman, P. K. Tucker, *Cladistics* **15**, 253 (1999).
33. J.-J. Jaeger et al., *Science* **286**, 528 (1999).
34. Supplemental data are available on Science Online at [www.sciencemag.org/cgi/content/full/294/5542/587/DC1](http://www.sciencemag.org/cgi/content/full/294/5542/587/DC1).

35. C. Ross, B. Williams, R. F. Kay, *J. Hum. Evol.* **35**, 221 (1998).
36. We are indebted to Nawab Mohammad Akbar Khan Bugti, Lord of the Bugti Tribes, and to Shahid Hassan Bugti for their total fieldwork assistance, to I. Akhund for his help, and to Bahadur Khan Rodani, Vice Chancellor of the University of Balochistan. We thank R. D. Martin for providing us useful comments on the manuscript. Many thanks to C. Denys and J. Cuisin (MNHN, Paris) for access to comparative material and to B. Marandat for preparing fossils. This work was funded by the University of Montpellier (CNRS-UMR 5554), the MNHN, Paris (CNRS-UMR 8569), the Fyssen, Leakey, Wenner-Gren, Singer-Polignac, Bleustein-Blanchet and Treilles Foundations. This is ISEM publication 2001-107.

9 August 2001; accepted 12 September 2001

## Caenorhabditis elegans p53: Role in Apoptosis, Meiosis, and Stress Resistance

W. Brent Derry,\* Aaron P. Putzke, Joel H. Rothman

We have identified a homolog of the mammalian p53 tumor suppressor protein in the nematode *Caenorhabditis elegans* that is expressed ubiquitously in embryos. The gene encoding this protein, *cep-1*, promotes DNA damage-induced apoptosis and is required for normal meiotic chromosome segregation in the germ line. Moreover, although somatic apoptosis is unaffected, *cep-1* mutants show hypersensitivity to hypoxia-induced lethality and decreased longevity in response to starvation-induced stress. Overexpression of CEP-1 promotes widespread caspase-independent cell death, demonstrating the critical importance of regulating p53 function at appropriate levels. These findings show that *C. elegans* p53 mediates multiple stress responses in the soma, and mediates apoptosis and meiotic chromosome segregation in the germ line.

The p53 tumor suppressor is among the most frequently mutated genes in human cancer and plays a critical role in maintaining genomic stability by regulating cell cycle progression and apoptosis in response to DNA damage (1, 2). Analysis of the mechanisms through which p53 integrates the cellular response to stress and damage in vivo has been limited by the absence of a genetic system. Recently, a p53 homolog was shown to participate in apoptosis induced by genotoxic stress in *Drosophila* (3–5) on the basis of forced expression of dominant negative forms; however, the organism-wide role of the gene could not be assessed in these experiments.

Standard searches of the genomic sequence suggested that *C. elegans* does not have a p53-like gene (6). However, using additional algorithms, we identified a *C. elegans* gene encoding a protein with signature sequences common to the p53 family, includ-

ing the residues most frequently mutated in human cancers (7). The cDNA sequence of this gene, *cep-1* (denoting *C. elegans* p53-like-1), predicts a 429-amino acid protein that is similar to the human protein in the NH<sub>2</sub>-terminal transactivation domain and the highly conserved DNA binding domains (Fig. 1). CEP-1 appears to be the only p53 family member encoded in the *C. elegans* genome, which suggests that p53 paralogs (including p63 and p73) may have evolved from a single ancestor related to CEP-1.

To assess the in vivo function of *cep-1*, we isolated a chromosomal rearrangement, *cep-1(w40)* (8). This mutant strain contains an intact copy of *cep-1* at its normal genomic location; the *cep-1(w40)* mutant gene, which encodes a truncated protein lacking the DNA binding domain, is translocated elsewhere in the genome. Although they exhibit impenetrant (~2%) embryonic lethality, *cep-1(w40)* mutants are generally viable and fertile. Moreover, depleting *cep-1* function by RNA interference (RNAi) (9) similarly leads to impenetrant embryonic lethality (Table 1). It is likely that RNAi results in a strong loss-of-function phenotype, as it eliminates detectable expression of a CEP-1::GFP

Department of Molecular, Cellular, and Developmental Biology, University of California, Santa Barbara, CA 93106, USA.

\*To whom correspondence should be addressed. E-mail: [derry@lifesci.ucsb.edu](mailto:derry@lifesci.ucsb.edu)

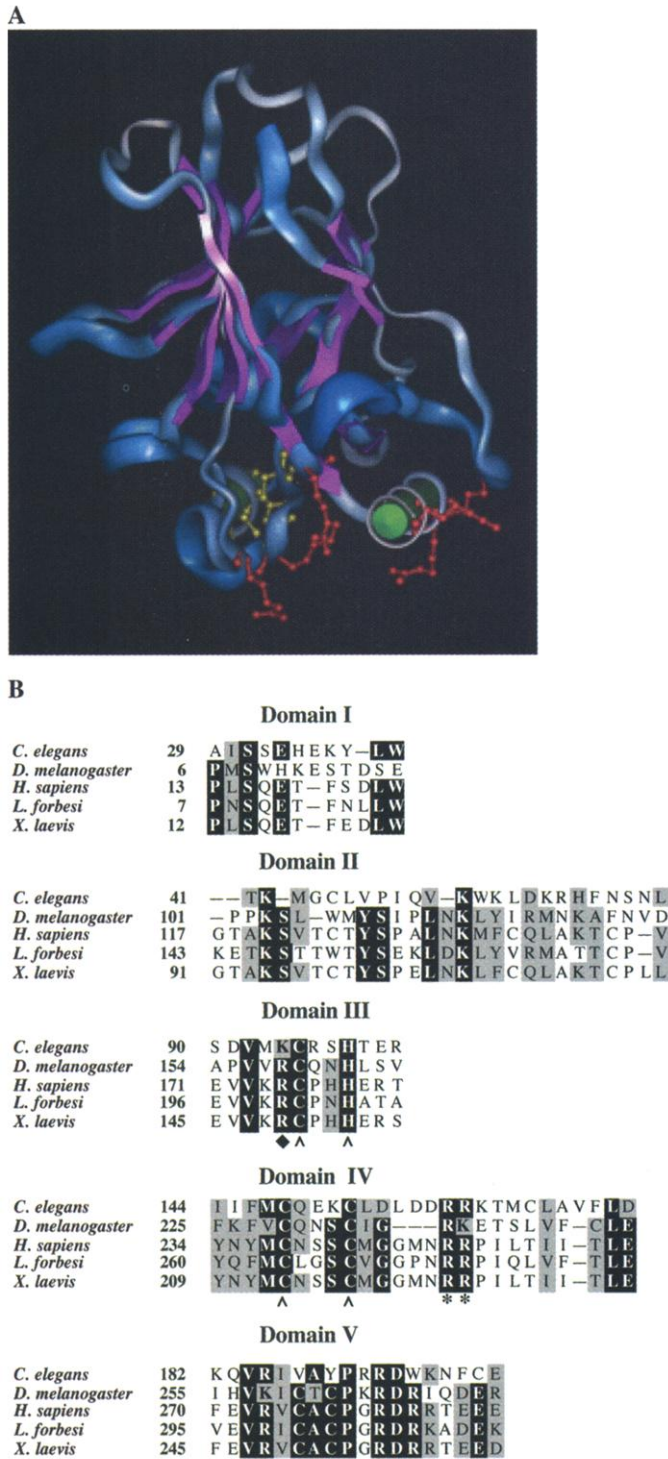
REPORTS

(green fluorescent protein) reporter (10). We found that both *cep-1(w40)* and *cep-1(RNAi)* embryos undergo a normal pattern of somatic apoptosis, suggesting that CEP-1 is not re-

quired for developmental programmed cell death in the soma (10).

Unlike somatic cells, which have a fixed cell division program, germ-line nuclei in *C.*

*elegans* undergo indeterminate rounds of division and are subject to checkpoint control and apoptosis in response to genotoxic stresses (11); they also undergo developmentally programmed "physiological" cell death, which appears to be regulated by distinct



of Mdm-2 with human p53 (35, 36). The region of highest conservation lies in the DNA binding domain (domains II to V), where several amino acids have been shown to contact the major and minor grooves of the p53 binding site in the DNA-p53 cocystal (34). These include four of the five most frequently mutated Arg residues in human cancer (asterisks), as well as Cys and His residues (carets) that make critical contacts with DNA in the three-dimensional structure of human p53. The fifth cancer "hot spot" Arg is conservatively substituted with a Lys in CEP-1 (diamond). The CEP-1 sequence corresponds to F52B5.5 reported by the *C. elegans* Sequencing Consortium (GenBank accession number CAA99857).

**Fig. 1.** Conservation of transactivation and DNA binding domains in *C. elegans* CEP-1. (A) Low-resolution three-dimensional model of CEP-1 DNA binding domain (residues 22 to 197) created with the program Modeller/Insight II 98.0 (33). The coordinates of residues 108 to 298 from the crystal structure of the human p53 DNA binding domain were used as the template (34). Conserved Arg residues that make contact with the consensus DNA binding site and that are the most frequently mutated residues in human cancer are shown in red. Amino acids in yellow represent conserved Cys and His residues that coordinate a Zn ion. Portions of the structure shown in magenta are the  $\beta$  strands of the core domain. The green rod indicates the H2 helix that makes contacts with the DNA. (B) Alignment of conserved domains in p53 family members. Single-letter abbreviations for amino acid residues are as follows: A, Ala; C, Cys; D, Asp; E, Glu; F, Phe; G, Gly; H, His; I, Ile; K, Lys; L, Leu; M, Met; N, Asn; P, Pro; Q, Gln; R, Arg; S, Ser; T, Thr; V, Val; W, Trp; and Y, Tyr.

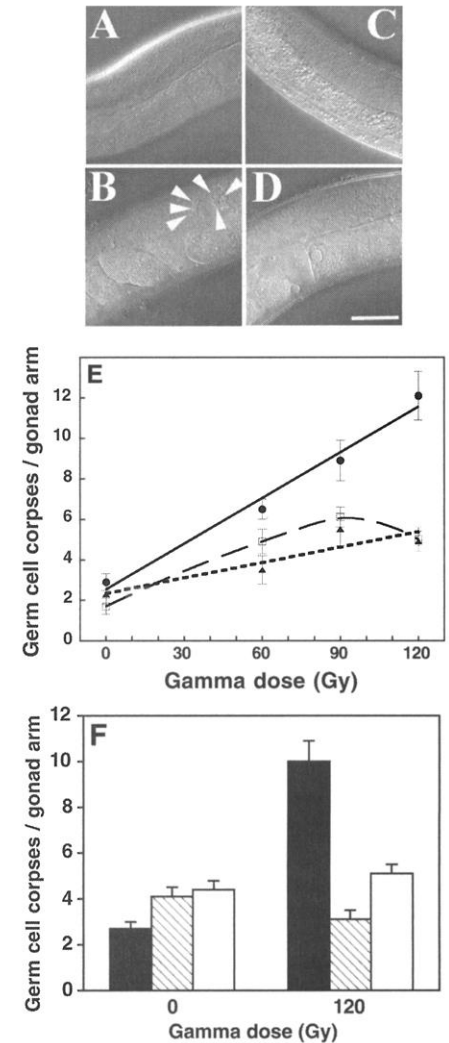


**Fig. 2.** Requirement of *cep-1* for normal activation of germ cell apoptosis in response to DNA damage. Shown are wild-type (A and B) and *cep-1(w40)* adults (C and D) observed by differential interference contrast (DIC) microscopy 12 hours after the L4 stage, either without radiation [(A) and (C)] or after exposure to 60-Gy IR [(B) and (D)]. Arrowheads point to germ cell corpses in a single focal plane. (E) Quantification of germ cell corpses with increasing doses of IR in wild-type (●), *cep-1(w40)* (▲), and *cep-1(RNAi)* adults (□). (F) Dominance of *cep-1(w40)* allele in suppressing DNA damage-induced germ cell apoptosis. Data are shown for wild type (solid bars), *cep-1(w40)/+* heterozygotes (hatched bars), and *cep-1(w40)/-* homozygotes (open bars) in the absence versus presence of 120-Gy IR. L4-stage hermaphrodites were irradiated with gamma rays from a <sup>137</sup>Cs source, and after 24 hours the number of apoptotic germ cells per gonad arm was determined in 10 to 15 animals. Error bars are SEM.

REPORTS

signaling pathways upstream of the core apoptotic machinery (12). DNA damage activates germ cell apoptosis through a conserved checkpoint pathway that includes the *rad-5* and *mrt-2* genes and the gene altered by the *op241* mutation; however, none of these genes is required for physiological germ cell death (11). Because p53 coordinates cellular responses to DNA damage, we hypothesized that *cep-1* might regulate apoptosis in the germ line in response to genotoxic stress. Indeed, *cep-1(w40)* hermaphrodites are resistant to ionizing radiation (IR)-induced apoptosis of germ cells (Fig. 2), and *cep-1(RNAi)* phenocopies this effect of *w40* (Fig. 2E). This block in activation of the germ-line cell death program may be general to DNA damage because *cep-1(w40)* mutants, like *rad-5*, *mrt-2*, and *op241* mutants (11), also fail to undergo germ cell death induced by the DNA modifying compound *N*-ethyl-*N*-nitrosourea (10).

Our observations suggest that the truncated CEP-1(w40) protein interferes with the

proapoptotic activity of wild-type CEP-1. Both a heterozygous *w40* mutation and overexpression of the *cep-1(w40)* gene from a heat shock promoter in a wild-type background confer resistance to IR-induced germ cell apoptosis, confirming that *w40* dominantly attenuates wild-type *cep-1* function (Fig. 2F) (10).

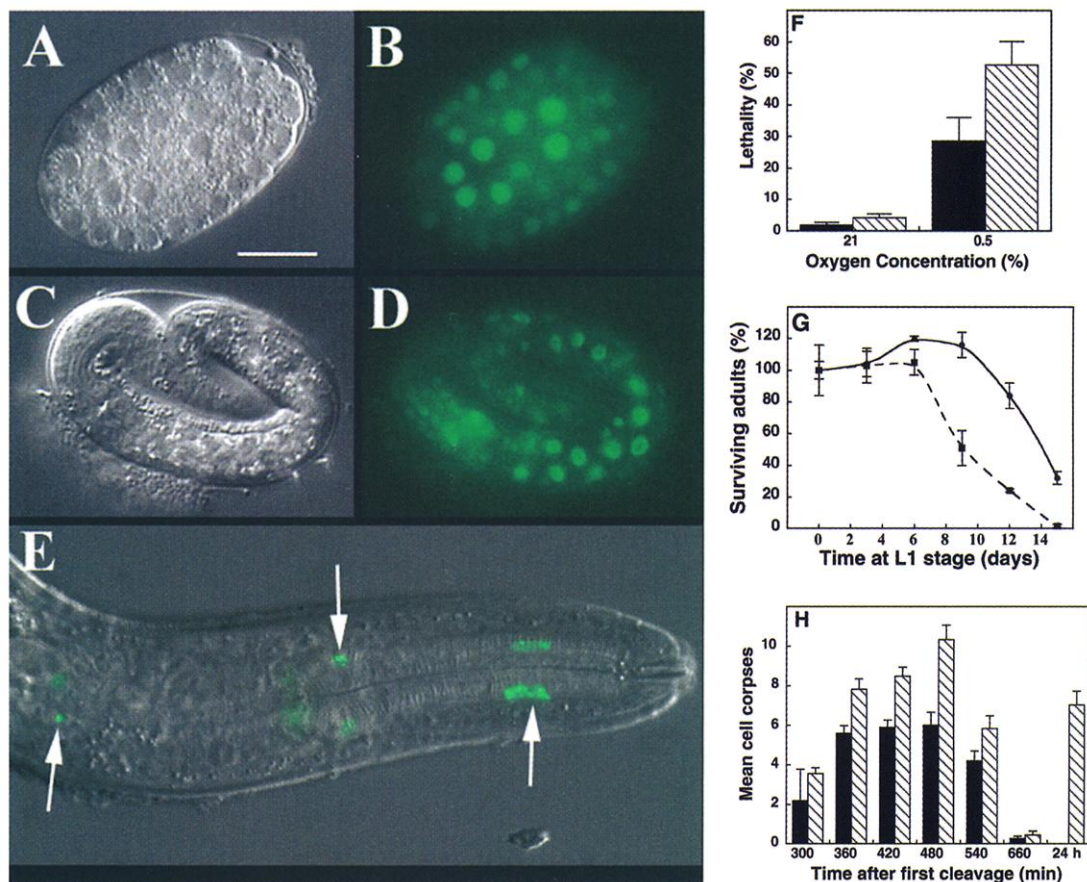
Unlike *rad-5*, *mrt-2*, and *op241* mutants, which are defective in both germ cell apoptosis and cell cycle checkpoint arrest induced by DNA damage, *cep-1(w40)* and *cep-1(RNAi)* germ cells undergo a transient cell cycle arrest in response to IR that is indistinguishable from that of the wild type (10). Furthermore, ectopic expression of CEP-1 in early embryos fails to cause cell division arrest. This ability to activate apoptosis but not arrest the cell cycle is a property shared by *Drosophila* p53, but not vertebrate homologs (3, 4), possibly revealing a primordial role for p53 proteins in apoptosis specifically.

Analysis of animals depleted for *cep-1*

function also uncovered a meiotic role in the absence of genotoxic stress. Nondisjunction of the X chromosome at meiosis I in the hermaphrodite germ line generates nullo-X gametes, leading to XO male progeny (13). We found that depletion of *cep-1* function by RNAi causes an increase in production of males (the Him phenotype, for high incidence of males) under normal growth conditions (Table 1). This effect was observed uniformly among broods of individual hermaphrodites, which implies that *cep-1* is required for chromosome segregation during meiosis rather than during the mitoses preceding meiosis. Mitotic proliferation of nuclei missing an X chromosome would be expected to produce much more variable broods, some with very high numbers of males. The *cep-1(w40)* mutant does not show a Him phenotype, which suggests that the truncated protein does not interfere with the meiotic chromosome segregation activity of CEP-1.

The low frequency of embryonic lethality in *cep-1* mutants (Table 1) might result from

**Fig. 3.** Expression and requirement of *cep-1* in somatic cells. (A to E) Zygotic expression pattern of a CEP-1::GFP fusion reporter in embryos and larvae. Shown are DIC (A and C) and fluorescence (B and D) images of embryos at ~50-cell (A and B) and pretzel (C and D) stages. Similar expression patterns were observed in six independent lines (10). Scale bar, ~10  $\mu$ m. (E) Overlay of GFP and DIC images of CEP-1 expression in pharynx after hatching. Anterior is to the right. Arrows point to nucleolar localization of CEP-1::GFP in anterior m2 muscle cells and other pharyngeal muscle and neurons of an L3-stage hermaphrodite. (F) Lethality of wild-type (solid bars) and *cep-1(w40)* embryos (hatched bars) under normoxic (21% O<sub>2</sub>) and hypoxic (0.5% O<sub>2</sub>) conditions. Early embryos were placed in chambers maintained with a constant atmosphere at the indicated oxygen concentration, as measured with a Systech oxygen analyzer. Lethality (percent  $\pm$  SEM) was scored by quantifying the number of surviving adults arising from a known number of embryos. (G) Effect of prolonged L1 starvation on survival to adulthood of *cep-1(w40)* (■) and wild-type larvae (●). Embryos were collected from gravid adults by hypochlorite treatment and hatched in M9 buffer with cholesterol (10  $\mu$ g/ml) at 20°C in the absence of food. Aliquots of arrested L1 larvae were taken every 72 hours and grown on NGM plates with OP50 bacteria. The fraction surviving to adulthood was determined after 3 days of growth at 20°C. We observed a slight increase in the number of



wild-type surviving adults between 6 and 9 days; this likely reflects sticking of some larvae to the culture tube at earlier time points. (H) Quantification of apoptotic death throughout embryonic stages after overexpression of wild-type CEP-1 (hatched bars) compared with overexpression of CEP-1(w40) (solid bars) by heat shock. Embryos between the 50- and 100-cell stage were collected from gravid adults and heat-shocked at 34°C for 15 min; cell corpses were quantified as the embryos developed. Error bars are SEM.

## REPORTS

autosomal meiotic nondisjunction or could reflect an essential function during normal embryogenesis. Consistent with the latter notion, we found that zygotic expression of a CEP-1::GFP fusion reporter is first detected at the ~50-cell stage and appears to be ubiquitous throughout embryonic development (14) (Fig. 3, A to D). Near the end of embryogenesis, GFP fluorescence decreases; after hatching, expression is restricted to a subset of pharynx cells, becoming concentrated in nucleoli (Fig. 3E).

Although little is known about the role of p53 in embryogenesis, knockout mice have revealed a role in normal development (15). p53 is also highly expressed embryonically in mice and frogs; however, its precise role during embryogenesis remains unclear (16–18). The high levels of ubiquitous CEP-1 expression in *C. elegans* might serve a protective function during embryogenesis, when cell division is rapid and replication errors are likely to occur at a higher frequency. However, *cep-1(w40)* embryos and larvae are not resistant to IR, the intensity and pattern of CEP-1::GFP expression does not change in response to this treatment, and the pattern of apoptosis in *cep-1(w40)* or *cep-1(RNAi)* embryos is indistinguishable from that of the wild type (10). Thus, the proapoptotic function of CEP-1 may be restricted to germ-line cells. Because somatic cells in *C. elegans* cannot generally be replaced if damaged, and arise by a determinate number of cell divisions (and hence are less likely to become tumorous), damage-induced apoptosis in the soma could be detrimental to the animal. In contrast, the germ line contains an excess of germ cells that are not used in self-fertilizing hermaphrodites, and damaged germ cells that are not eliminated could result in defective progeny, making it desirable to eliminate these expendable cells.

Because the DNA damage checkpoint function of CEP-1 is apparently restricted to the germ line, we reasoned that somatic CEP-1 might instead activate a response to other stresses. In vertebrates, p53 is activated by diverse stress signals, including hypoxia,

which leads to stabilization of the protein (19, 20). As a soil-dwelling nematode, *C. elegans* is likely to encounter hypoxic environments frequently. Indeed, we found that *cep-1(w40)* mutants are hypersensitive to the lethal effects of hypoxia (Fig. 3F).

Under conditions of starvation stress, *C. elegans* first-stage (L1) larvae undergo developmental arrest until food is available. We found that the life-span of *cep-1(w40)* larvae is reduced relative to the wild type when they were starved at the L1 stage (Fig. 3G). Wild-type survival was reduced by 50% after ~14 days, whereas survival of *cep-1(w40)* larvae was reduced by the same magnitude after only ~9 days (Fig. 3G). In contrast, we found that the life-span of mutant animals during normal growth was unaffected (10). The effect of starvation- and hypoxia-induced stress on *cep-1* mutants suggests that CEP-1 can modulate responses to both genotoxic stress in the germ line and environmental stress in the soma.

To address the importance of maintaining proper CEP-1 levels during development, we overexpressed CEP-1 from a heat shock-inducible promoter in 50- to 100-cell-stage embryos (21). The resultant embryos often arrested before hatching and showed severe morphological abnormalities. These embryos did not undergo cell cycle arrest, but they showed a significant increase in the number of cell corpses that accumulated throughout embryogenesis; some terminally arrested embryos contained as many as 40 cell corpses (Fig. 3H) at a time when wild-type animals contain virtually none. No apoptotic corpses were observed when CEP-1 was overexpressed in a mutant lacking CED-3 caspase function (10), which is required for all developmentally programmed cell deaths (22). CEP-1-overexpressing embryos that underwent apparently normal development, and that did not show significantly elevated numbers of cell corpses, nevertheless invariably succumbed, arresting before hatching or as L1 larvae with widespread signs of necrosis. Indeed, overexpression of CEP-1 at all larval stages and during adulthood also caused pen-

etrant lethality and widespread necrotic cell death, independent of CED-3 caspase function. All larvae overexpressing the protein became uncoordinated within 8 hours after induction of *cep-1* overexpression and eventually degenerated.

The lethality of overexpressed CEP-1 appears to be a specific effect, as it requires an intact DNA binding domain; overexpression of the truncated *cep-1(w40)* allele resulted in virtually no effect on viability. Moreover, we found that expression of human p53 results in similar degenerative phenotypes in *C. elegans* embryos and larvae (10), which suggests that human p53 and nematode CEP-1 can perform similar biochemical functions. The lethality of overexpressed *cep-1* does not appear to result from activation of the core apoptotic machinery, because mutations in *ced-3* or *ced-4* (22) did not block these effects (10). However, dying animals contained large numbers of nuclei that stained positive for acridine orange, generally regarded as a marker of apoptosis (23). Therefore, high levels of CEP-1 may override the requirement for the CED-3 caspase and activate a caspase-independent cell death program, perhaps analogous to the caspase-independent apoptosis observed recently in other systems, which is revealed when caspase function is blocked in cells otherwise programmed to die (24).

We find that *C. elegans* p53 functions both during normal development (e.g., to ensure proper meiotic chromosome segregation) and under conditions of cellular and genotoxic stress (e.g., in response to DNA damage, hypoxia, or starvation). Although it is expressed ubiquitously in embryos, *cep-1* must be carefully regulated because elevated levels of CEP-1 protein are invariably lethal. It should now be possible to use *C. elegans* as a genetic system to screen for modifiers of the *cep-1* mutant phenotype, allowing a comprehensive dissection of the pathways through which p53-like proteins function to mediate stress response, to activate germ-line apoptosis, and to regulate meiotic chromosome segregation.

**Table 1.** Elimination of *cep-1* function causes meiotic X chromosome nondisjunction.

Genotype	Total F <sub>1</sub> 's	Total dead eggs	Percent dead eggs	Total males*	Percent males
<i>unc-22(RNAi)</i> †	3971	32	0.8	2	0.1
<i>cep-1(RNAi)</i> †	2355	113	4.8	33	1.4
N2‡	2464	2	0.08	4	0.2
<i>cep-1(w40)</i> ‡	2886	38	1.2	10	0.3

\*Males produced by *cep-1(RNAi)* hermaphrodites mated normally and produced the expected frequency of male cross progeny (10), implying that CEP-1 is needed for a function in normal meiotic chromosome segregation and not for sexual identity per se. †Between 15 and 20 L4-stage N2 hermaphrodites were soaked in *cep-1* double-stranded RNA (~5 mg/ml) for 16 to 18 hours at 20°C. Soaked adults were transferred every 24 hours, and dead eggs, males, and hermaphrodites were scored in the F<sub>1</sub> generation. *unc-22(RNAi)* was used as a negative control; although this RNAi treatment invariably results in a penetrant *Unc-22* phenotype, no significant effect on male production or viability was seen. ‡N2 (wild-type) and *cep-1(w40)* strains were soaked in M9 buffer for 16 to 18 hours at 20°C and scored as described above.

## References and Notes

- A. J. Levine, *Cell* **88**, 323 (1997).
- L. J. Ko, C. Prives, *Genes Dev.* **10**, 1054 (1996).
- M. Ollmann et al., *Cell* **101**, 91 (2000).
- M. H. Brodsky et al., *Cell* **101**, 103 (2000).
- S. Jin et al., *Proc. Natl. Acad. Sci. U.S.A.* **97**, 7301 (2000).
- G. M. Rubin et al., *Science* **287**, 2204 (2000).
- The amino acid sequence of squid (*Loligo forbesi*) p53 (U43595) was used as a query to search the *C. elegans* database with the PSI-BLAST algorithm (25). Several low-scoring *C. elegans* open reading frames were identified and aligned with several p53 family members using the Block Maker tool (26). F52B5.5 was the only predicted *C. elegans* gene identified with the appropriate p53 signature sequences in the correct modular order. There are seven exons in *cep-1*, and the intron-exon boundaries are in similar positions to those in the murine and human

p53 genes (27, 28), underscoring their evolutionary relatedness.

8. We screened 48,000 wild-type (N2) genomes for a *cep-1* deletion using 4,5',8-trimethylpsoralen/ultraviolet light mutagenesis as described (29, 30). First-round polymerase chain reaction primers flanking *cep-1* were 5'-GGTGGACTGTTCGCTTGAATCAA-GACTGC-3' and 5'-GCTCTTGATGTGCCAACAA-GATCGGATTC-3'. Second-round primers were 5'-CAGGGGAGTTGGCGTTAGG-3' and 5'-AATTGGTA-CAGCGACTTCTCTTCA-3'. A single worm containing the *cep-1(w40)* deletion was identified. This deletion removes 1823 nucleotides of the gene, corresponding to nucleotides 28,754 to 31,967 on cosmid F52B5. The splice acceptor and donor sites remain intact in the *cep-1(w40)* allele, which is predicted to encode an in-frame but truncated protein missing amino acids 69 to 242. Further analysis showed that the deletion strain also carries an intact copy of *cep-1*. The *w40* allele segregates independently of the wild-type *cep-1* locus, indicating that the deleted copy had translocated to another region of the genome and a wild-type copy of *cep-1* remains at the normal locus.
9. A. Fire *et al.*, *Nature* **391**, 806 (1998).
10. W. B. Derry, J. H. Rothman, unpublished data.
11. A. Gartner, S. Milstein, S. Ahmed, J. Hodgkin, M. O. Hengartner, *Mol. Cell* **5**, 435 (2000).
12. T. L. Gumienny, E. Lambie, E. Hartweig, H. R. Horvitz, M. O. Hengartner, *Development* **126**, 1011 (1999).
13. D. G. Albertson, A. M. Rose, A. M. Villeneuve, in *C. elegans II*, D. L. Riddle, T. Blumenthal, B. J. Meyer, J. R. Priess, Eds. (Cold Spring Harbor Laboratory Press, Cold Spring Harbor, NY, 1997), pp. 47-78.
14. To determine the expression pattern of *cep-1*, we designed a reporter construct that includes 4.5 kb of sequence upstream of the start codon as well as the entire CEP-1 coding sequence, fused in-frame to GFP. The *cep-1* sequences were obtained by amplification from cosmid F52B5 and cloned into vector pPD 96.04. Reporter constructs were coinjected with the dominant *rol-6(su1006)* marker gene to create transgenic lines (31). This results in repetitive arrays that are generally silenced in the germ line; thus, the marker is likely to reveal the zygotic expression exclusively.
15. T. Jacks *et al.*, *Curr. Biol.* **4**, 1 (1994).
16. A. Rogel, M. Popliker, C. G. Webb, M. Oren, *Mol. Cell Biol.* **5**, 2851 (1985).
17. P. Schmid, A. Lorenz, H. Hameister, M. Montenarh, *Development* **113**, 857 (1991).
18. J. B. Wallingford, D. W. Seufert, V. C. Virta, P. D. Vize, *Curr. Biol.* **7**, 747 (1997).
19. T. G. Graeber *et al.*, *Mol. Cell Biol.* **14**, 6264 (1994).
20. R. Alarcón, C. Koumenis, R. K. Geyer, C. G. Maki, A. J. Giaccia, *Cancer Res.* **59**, 6046 (1999).
21. Genomic *cep-1* was amplified from cosmid F52B5 using primers tagged with a Kpn I site 5' of the ATG start codon and a Sac I site after the stop codon and cloned into vectors pPD 49.78 (*hsp16-2*) and pPD 49.83 (*hsp16-41*). Transgenic lines were established by standard methods (31). The primers were 5'-GCGGTACCATGAATTTGAATGAAGATTG-3' and 5'-CCGAGCTCTACTTTGGCAGTTTCATCG-3'. CEP-1 was overexpressed in transgenic worms by subjecting them to a 15- to 20-min heat shock at 34°C (32).
22. H. M. Ellis, H. R. Horvitz, *Cell* **44**, 817 (1986).
23. J. M. Abrams, K. White, L. I. Fessler, H. Steller, *Development* **117**, 29 (1993).
24. C. Kitahara, Y. Kuchino, *Cell Death Differ.* **6**, 508 (1999).
25. S. F. Altschul *et al.*, *Nucleic Acids Res.* **25**, 3389 (1997).
26. S. Henikoff, J. G. Henikoff, W. J. Alford, S. Pietrokovski, *Gene* **163**, 17 (1995).
27. B. Bienz, R. Zakut-Houri, D. Givol, M. Oren, *EMBO J.* **3**, 2179 (1984).
28. P. Lamb, L. Crawford, *Mol. Cell Biol.* **6**, 1379 (1986).
29. G. Jansen, E. Hazendonk, K. L. Thijssen, R. H. A. Plasterk, *Nature Genet.* **17**, 119 (1997).
30. K. Gengyo-Ando, S. Mitani, *Biochem. Biophys. Res. Commun.* **269**, 64 (2000).
31. C. C. Mello, J. M. Kramer, D. Stinchcomb, V. Ambros, *EMBO J.* **10**, 3959 (1991).

32. E. G. Stringham, D. K. Dixon, D. Jones, E. P. M. Candido, *Mol. Biol. Cell* **3**, 221 (1992).
33. A. Sali, T. L. Blundell, *J. Mol. Biol.* **234**, 779 (1993).
34. Y. Cho, S. Gorina, P. D. Jeffrey, N. P. Pavletich, *Science* **265**, 346 (1994).
35. J. Lin, J. Chen, B. Elenbaas, A. J. Levine, *Genes Dev.* **8**, 1235 (1994).
36. C. J. Thut, J. L. Chen, R. Klemm, R. Tjian, *Science* **267**, 100 (1995).
37. We thank M. Fukuyama for help with the deletion screen, C. Farmer and the Tri-Counties Blood Bank for use of their gamma source, R. Christoffersen for hypoxic chambers, S. Roberts for providing the three-dimensional model, R. Halberg for useful discussions,

A. Fire for vectors, and A. Coulson for cosmid. Some of the strains were provided by the *Caenorhabditis* Genetics Center, which is funded by the National Center for Research Resources of NIH. Supported by the Cancer Center of Santa Barbara and the Tri-Counties Blood Bank (W.B.D.) and grants from Santa Barbara Cottage Hospital, the University of California Cancer Research Coordinating Committee, and National Institute on Aging grant AG13736 (J.H.R.).

17 August 2001; accepted 3 September 2001  
 Published online 13 September 2001;  
 10.1126/science.1065486  
 Include this information when citing this paper.

# Integration Between the Epibranchial Placodes and the Hindbrain

Jo Begbie and Anthony Graham\*

Developmental integration results from coordination among components of different embryonic fields to realize the later anatomical and functional relationships. We demonstrate that in the chick head, integration between the epibranchial placodes and the hindbrain is achieved as the neuroglial hindbrain crest cells guide the epibranchial neuronal cells inward to establish their central connections. This work defines a role for the neuroglial hindbrain crest in organizing the afferent innervation of the hindbrain.

After regional specification, during which constituent parts of an embryonic field are defined, the next developmental challenge is that of integration, during which the different embryonic fields are coordinated, and thus, later anatomy and function established. Developmental integration is particularly apparent in the vertebrate head, because head development involves integration of a number of disparate embryonic cell types (1). Here, we studied in the chick the development of the epibranchial ganglia: the geniculate, petrosal, and nodose, which convey gustatory and viscerosensory information from the oro-pharyngeal cavity to central sensory nuclei in the hindbrain (Fig. 1, A and B) (2). The sensory neurons of these ganglia originate in the epibranchial placodes and connect to the central nervous system (CNS) (3, 4). These placodes are focal thickenings of ectoderm close to the tips of the pharyngeal pouches, and which are induced by the pharyngeal endoderm through the action of Bmp-7 (5). It has been unclear, however, how the neuronal cells generated by the epibranchial placodes migrate internally to the site of ganglion formation. We show here that this process is mediated by the neuroglial rhombencephalic neural crest. The epi-

branchial neuronal cells move inward along the tracks of neuroglial neural crest that extend from the hindbrain to the placodes. These results define a role for the neuroglial hindbrain neural crest in the integration of hindbrain and epibranchial placode development.

With a view toward understanding this process, we characterized the migratory paths taken by the epibranchial placodal cells as they move internally. The placodal cells were labeled by application of the lipophilic dye DiI to the exterior of the embryo, at stages concomitant with the induction of these placodes (6). This procedure results in the labeling of the embryonic ectoderm. Cells that leave this tissue layer carry the label with them as they move inward (Fig. 1). Cells migrating from both the geniculate and the petrosal placodes form organized streams extending from the placodal ectoderm toward the hindbrain (Fig. 1).

The migratory paths formed by the epibranchial neuronal cells are reminiscent of those formed by another group of cells, the neural crest. The neural crest cells in this region of the embryo migrate as segregated streams from specific axial levels of the hindbrain (Fig. 2A) (7, 8). The crest cells within these streams, however, have two distinct fates. The early ventrally migrating population fill the underlying pharyngeal arches and form ectomesenchymal derivatives within these structures, whereas the

Medical Research Council (MRC) Centre for Developmental Neurobiology, Fourth Floor, New Hunts House, Guys Campus, Kings College London, London SE1 9RT, UK.

\*To whom correspondence should be addressed. E-mail: anthony.graham@kcl.ac.uk